



**FRIEDRICH-SCHILLER-
UNIVERSITÄT
JENA**

BACHELOR THESIS

Faculty of Chemistry and Earth Sciences
Friedrich-Schiller-University Jena

Energy and water controls of Sun-Induced Fluorescence extremes

for the attainment of the academic degree
Bachelor of Science

written by

Josephin Kroll

matriculation number: 160443

born in Gotha, 11-29-1996

January 2021

First examiner: Prof. Dr. Anke Hildebrandt
Second examiner: Dr. René Orth

Acknowledgements

First of, I would like to thank Prof. Dr. Anke Hildebrandt for introducing me to the topic of ecohydrology and building up my enthusiasm for it.

Many thanks I want to give to Dr. René Orth for including me into the department for Biogeochemical Integration at the Max-Planck-Institute for Biogeochemistry, especially the Hydrology-Biosphere-Climate Interactions group. I am really grateful for the appreciative work-environment you create, the idea of this topic and all your feedback and contributions. Particularly, I want to thank Jasper Denissen for giving constructive feedback over and over again, when I needed support in writing, giving talks and coding, and of course for all the great array names. Also, many thanks to Wantong Li, your study was a great inspiration and your feedback and comments improved this one. Thanks to all of you, it felt for me like co-working and not like having to proof my skills to someone.

At the end, I want to thank Juliane Beuster for proofreading my thesis and hearing the same talks for many times. Thanks to her and other people for always cheering me up.

Contents

List of abbreviations	3
List of Figures	5
1 Introduction	6
2 Data and Methods	8
2.1 Data	8
2.2 Data Processing	9
2.3 Climate characteristics	11
3 Results	13
3.1 Development of hydro-meteorological variables around extreme vegetation productivity	13
3.2 Global maps	14
3.3 Temperature-aridity plots, dominant variable	16
3.4 Temperature-aridity plots: second dominant variable	19
3.5 Difference between dominant and second-most represented variable	20
4 Discussion	23
4.1 Developments of hydro-meteorological variables before and after extreme vegetation productivity	23
4.2 Global maps	24
4.3 Temperature-aridity plots	26
4.4 Second-most dominant variable and differences to the dominant variable	28
5 Conclusion	29

List of abbreviations

- SIF: Sun-Induced Chlorophyll Fluorescence
- VPD: vapor pressure deficit
- SSRD: surface solar radiation downwards, referred to as radiation
- ssr: surface net solar radiation
- str: surface net thermal radiation
- t2m, temp: temperature in 2 m height
- tp: total precipitation, referred to as precipitation
- SM1-4: soil moisture, number indicates the layer, which is referred to
- AI: aridity index
- ET: evapotranspiration
- FVC: fractional vegetation cover

List of Figures

1	Data processing.	10
2	Months of extreme events.	11
3	Development of SIF and variables before and after the vegetation productivity extreme.	14
4	Dominant hydro-meteorological variable and its magnitude during extreme vegetation productivity.	16
5	Temperature-aridity plots for extreme vegetation productivity. . .	18
6	Temperature-aridity plots for extreme vegetation productivity, second most represented hydro-meteorological variable.	21
7	Difference between percentage of grid cells with most represented variable and second-most represented variable.	22
8	Dominant variables for average vegetation productivity.	26
9	Temperature-aridity plot of the controlling variables for average vegetation productivity.	28
10	First and second dominant variables in various climates conditions and the difference between percentages of grid cells representing them.	30

1 Introduction

Biosphere has a crucial role in the earth system, as it connects the water with the carbon cycle. Through photosynthesis, which is sequestering carbon and at the same time transpiring water, vegetation productivity is closely linked with both cycles. Vegetation as part of the biosphere is influenced by different characteristics: soil properties, carbon content in the atmosphere, available water and energy. Vegetation interacts in the water cycle through evapotranspiration (ET), transporting water from the soil to the atmosphere. As preserving the carbon cycle, also gross primary production is used as a proxy for vegetation functioning. There are several studies determining the main limitations of ET, stating that they are mainly dependent on the dryness of the region. In dry regions ET is limited by water, where in wet regions energy has a limiting effect (Denissen et al. 2020; Seneviratne et al. 2010).

A satellite observed proxy for vegetation productivity is Sun-induced Chlorophyll Fluorescence (SIF) (Joiner et al. 2013). With this data, it can be identified, where, when and to what extent vegetation is being productive. This allows the combining of e.g. hydro-meteorological variables with vegetation productivity. Several studies investigate the influence of climate extremes like droughts and/or heatwaves on vegetation functioning using SIF as its proxy (Zhang et al. 2019; Qiu et al. 2020; Xiaorong Wang et al. 2019). Herein, SIF-limiting variables are mainly considered as precipitation and temperature, each study chooses additionally a few other variables, e.g. radiation, soil moisture. Besides, W. Li et al. 2020 and X. Li and Xiao 2020 analyzed how long-term average global vegetation productivity is influenced by different variables. W. Li et al. 2020 emphasize the importance of the variety of considered hydro-meteorological variables, when investigating vegetation productivity. Additionally, it is deduced that vegetation productivity in arid regions is water-controlled, while energy variables are the main drivers in humid regions. This confirms the before mentioned findings of Denissen et al. 2020; Seneviratne et al. 2010.

Hence, there is increasing knowledge about climate extremes influencing vegetation and long-term controls of its productivity. Nevertheless, vegetation productivity extremes themselves were not yet focus of investigations. There is a lack of information about co-variations between hydro-meteorological variables and maximum or minimum vegetation productivity. Processes leading to those vegetation productivity extremes should be known, so that occurring mechanism can be analysed and better understood. Additionally, knowing about the supportive or

inhibiting character of variables associated with vegetation productivity is relevant in terms of securing food production and several economic interests like crop yields and forest management. Therefore, this study aims to detect anomalies of vegetation productivity and to determine, which hydro-meteorological variables can be associated with these occurrences. From here, possible shifts from energy- to water-limitation can be derived when contrasting average to extreme vegetation productivity.

2 Data and Methods

In section 2.1 the data, which was used for the study is described. Section 2.2 explains the data processing and in section 2.3 the used climate characteristics are introduced.

2.1 Data

Sun - Induced Chlorophyll Fluorescence is used from satellite data of the Global Ozone Monitoring Experiment-2 (GOME-2) project (Köhler, Guanter, and Joanna Joiner 2015). To account for small-scale noise in both time and space, SIF is used at a monthly time scale and $0.5^\circ \times 0.5^\circ$, which equals $110.6 \text{ km} \times 111.3 \text{ km}$ at the equator to $111.7 \text{ km} \times 19.4 \text{ km}$ at a latitude of 80° . As energy variables radiation, temperature and vapor pressure deficit (VPD) are considered, highlighting different mechanisms affecting vegetation productivity. Water variables contain of soil moisture in different layers (SM layer 1 (0-7cm), layer 2 (7-28 cm), layer 3 (28-100 cm) and layer 4 (100-289 cm)) and total precipitation. Precipitation, vapor pressure deficit (VPD), temperature and radiation from ERA5 data are used at a spatial scale of $0.5^\circ \times 0.5^\circ$, and on a monthly basis ((C3S) 2017). Multi-layer soil moisture (SM) data has the same spatial resolution, but in contrast is only available at a daily time scale. Thus, the daily values are aggregated to monthly means.

Table 1: Data used in this study.

Data set	Version	Variables	Spat. res.	Temp. res.	derived from	Reference
GOME-2	GFZ	Sun-induced Chlorophyll Fluorescence (SIF) _v	$0.5^\circ \times 0.5^\circ$	Monthly	Satellite observations	Köhler, Guanter, and Joanna Joiner 2015
ERA5		tp, ssrd, t2m, vpd	$0.5^\circ \times 0.5^\circ$	Monthly	Reanalysis model	(C3S) 2017
ERA5		swvl1-4, ssr, str, tp	$0.5^\circ \times 0.5^\circ$	Daily	Reanalysis model	(C3S) 2017
FVC		FVC	$0.5^\circ \times 0.5^\circ$			Hansen 2018

2.2 Data Processing

The data processing, which is also illustrated in fig. 1 is applied to SIF and the hydro-meteorological variables. Every graph shows a time series for a grid cell with the coordinates 5°W, 41.5°N (Northwest Spain) from 2007 - 2015 and is illustrating one of the processing steps.

The focus of this analysis is on variation of anomalous vegetation productivity, which cannot be explained through the seasonal cycle. To eliminate its influence, anomalies function as meaningful values. As these are calculated out of the initial SIF data, long-term trends of the data set could be carried over into them and influence the detected extremes. To prevent this, the data has to be detrended. Using a linear model, the trend of SIF values over the whole study period is calculated. The received slope is subtracted from the initial monthly values, resulting in a detrended time series. The effect can be seen in fig. 1b and fig.1c. In order to calculate the anomalies, the mean monthly seasonal cycle is subtracted from the detrended time series.

On the resulting time series (fig. 1d) three kinds of filtering are applied to secure that grid cells with hardly any or no vegetation are excluded. The filtering methods are adopted from the study of (W. Li et al. 2020) to enable the comparison of results. First of all, anomalies of months with an initial SIF value below $0.5 \text{ MW m}^{-2} \text{ sr}^{-1} \text{ nm}^{-1}$, which is related to hardly any vegetation productivity, are filtered. If after that, a grid cell has less than 16 monthly values, all remaining ones are removed. The last step is to keep only grid cells with a fractional vegetation cover (FVC) larger than 5% (FVC data from Hansen 2018), effectively excluding grid cells with hardly any vegetation. The remaining data (fig. 1e) is used to determine the three highest and lowest anomalies in the whole time series, which represent maximum (blue) and minimum (red) vegetation productivity (fig. 1f). Additionally, the extreme with the highest magnitude is separated. A number of three vegetation productivity maxima/minima ensures that co-occurring anomalies of hydro-meteorological variables are not purely coincidental. Further, considering more SIF maxima/minima might include less extreme ones.

After processing the data, both maximum and minimum vegetation productivity are expected to occur in periods that have on average high productivity, as in periods of high average productivity variability is highest. To determine at what month-of-year the highest/lowest vegetation productivity occurred, the month in which they are detected is plotted (fig. 2). In the northern hemisphere, where growing season is mostly during April - September, the displayed months of maximum

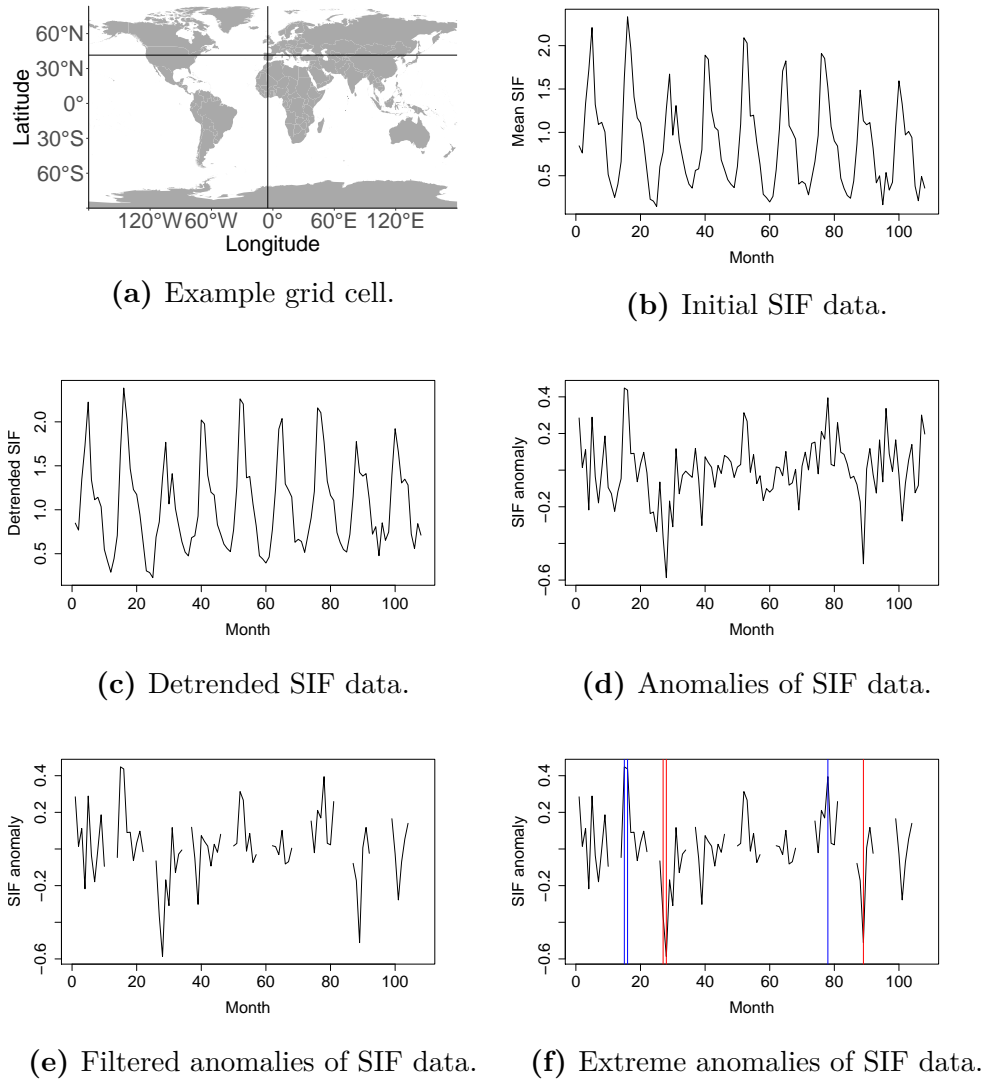


Figure 1: Processing of the initial SIF data from 2007 - 2015. a) Localisation of the example grid cell, indicated by the crossing of black lines. b) Long-term variation of initial SIF values, c) detrended SIF data, d) calculated SIF anomalies and e) filtered SIF anomalies over the whole time series. f) Long-term variation of filtered SIF anomalies, blue lines indicate the three maximum SIF events, red lines indicate the minimum SIF events.

and minimum vegetation productivity range within this period. In contrast, the southern hemisphere vegetation is most active during October - March, what is in line with the months displayed for extreme vegetation productivity. In summary, minima and maxima occur in the growing season as expected.

Additionally, the filtering method causes regions with coarse vegetation, to be filtered from the analysis and therefore no data to display is available, e.g. in

northern Russia and the Poles.

The anomalies of the hydro-meteorological variables are computed like described for the SIF data. As a final step, they are normalized to receive comparable magnitudes of all variables. Therefore, the standard deviation is calculated over the nine years for each of the twelve months. After that, the anomalies of every month are divided by their standard deviation, which rids the variables of their respective units, now expressed in standard deviations and therefore comparable.

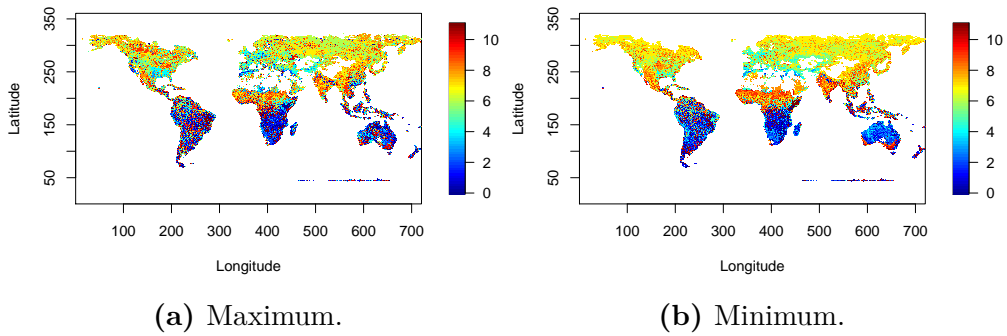


Figure 2: Global map indicating the months in which extreme SIF events occurred.

2.3 Climate characteristics

Grid cells are characterized by their long-term average temperature and aridity index (AI) to define certain climate types, between which can be distinguished. To calculate the long-term average temperature for a grid cell, daily temperature values are averaged over the whole time period. Temperature levels range from -10°C to 40°C in intervals of 10. Regions with a mean long-term temperature above 10°C are referred to as warm, below this threshold they are considered as cold.

To compute the aridity index, long-term means of net radiation are divided by long-term means of precipitation, resulting in a dimensionless ratio. The data for precipitation and radiation is from ERA5 on a daily time scale with a spatial resolution of $0.5^{\circ} \times 0.5^{\circ}$ ((C3S) 2017). As the AI is thought as ratio of evapotranspiration to precipitation, a value higher than 1 needs evaporation to be larger than the water available through precipitation, what accounts for arid regions. The opposite accounts for humid regions, where precipitation needs to provide more water than what can be lost through evapotranspiration. Of course, there are transitional regimes, where partly arid, partly humid conditions prevail.

In this study five aridity classes are chosen: 0-0.5, 0.5-1, 1-2, 2-4, 4-8. To address the different AIs, regions with an $AI > 0.5$ are considered as humid, $0.5 < AI < 1$ as semihumid, $1 < AI < 2$ as semiarid and > 2 as arid.

3 Results

3.1 Development of hydro-meteorological variables around extreme vegetation productivity

As described in 2.2 the largest positive and negative anomalies of SIF values are determined per grid cell to detect extreme vegetation productivity. To compare the SIF extremes together with hydro-meteorological variables, the normalized anomalies of SIF are used. The data are collected during extreme vegetation productivity as well as two months before and after, resulting in a time series of five months. The illustration 3 gives an idea about the onset and legacy of the vegetation extreme and the hydro-meteorological variables. The course of energy and water controls can be used to derive possible hypotheses about interactions with vegetation productivity. The development is shown for maximum and minimum events in Germany and on the Iberian Peninsula. The two locations are chosen because of their different climate conditions. Central Germany has an AI = 0.84 and a mean long-term temperature of 8.85 °C. The climate of the northwest Spain is characterized by an AI = 2.06, with an average temperature of 12.95 °C. Where the SIF magnitude is highest in Germany, VPD and temperature decrease but remain within the positive range. In contrast, soil moisture in layer 1-3 is lower than usual but increasing. Additionally, a strong increase of precipitation leads to a weakly positive anomaly. However, soil moisture in layer 4 as well as radiation decrease, reaching their average values during the vegetation productivity maximum. Similarities can be found in fig 3b. Vegetation productivity co-variates with decreasing VPD and temperature, where radiation is on its average range. Water variables are increasing (except for soil moisture 4), but below their mean values.

The minimum vegetation productivity is illustrated by the fig. 3c and 3d. The two graphs display what is suggested in the hypothesis regarding humid regions being energy controlled and arid regions, where water variables prevail. In Germany the vegetation productivity minimum is accompanied by low radiation and VPD but high amounts of soil moisture in all layers. In contrast, on the Iberian Peninsula the vegetation productivity minimum is associated by extreme low soil moisture, especially in the surface layers. Deep soil moisture is general extreme low during the whole time period. One month before the vegetation productivity minimum emerges, there is an energy surplus, VPD, radiation and temperature show high positive anomalies. In the month of the minimum vegetation productivity,

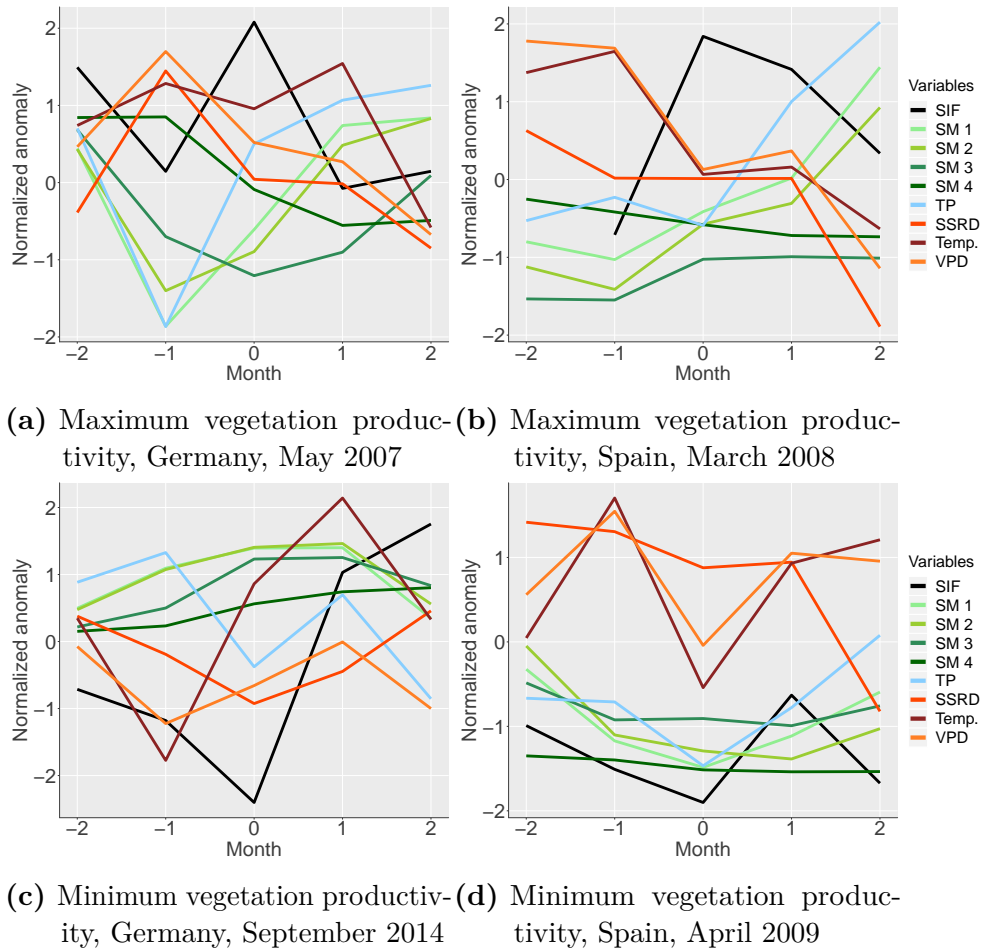


Figure 3: Development of SIF and hydro-meteorological variables before and after extreme vegetation productivity, which is displayed at month = 0.

radiation is still higher than usual, whereas VPD and temperature decrease, resulting in average or even negative anomalies.

3.2 Global maps

After determining the three highest and lowest SIF events, the normalized anomalies of hydro-meteorological variables are averaged, thereby obtaining robust estimates of these variables over three maxima and minima. The resulting eight values per extreme can be sorted by their magnitude. An example is given in tab. 2. It is assumed that the variable with the largest normalized anomaly is exerting the largest influence on vegetation productivity. To create a global map of the dominant variables, every grid cell is colored in the specific color of its dominant variable. Additionally, the normalized anomalies of the dominant variables are plotted, where the magnitude of the value is indicated by a color ramp. The aim

here is to create an impression, where surpluses and where deficiencies of water or energy occur.

Table 2: Mean value of normalized anomalies of each variable during three minimum SIF events for a grid cell in central Germany.

SSRD	Temp	VPD	SM1	SM2	SM3	SM4	TP
-0.95	-0.29	-0.62	0.73	0.70	0.50	-0.10	0.12

The described visualisation process creates the global maps in fig. 4. Comparing fig. 4a and 4b, both appear similar regarding the regions where water or energy prevails. Vegetation above 60°N seems mainly energy controlled, whereas below soil moisture is dominant. Especially, in the region of north Asia the border between energy and water limitation is clearly visible.

Below 45°N both maps are quite noisy. However, for the vegetation productivity maximum, one could detect a few, weak spatial patterns. In Mexico, east Africa and central Australia soil moisture in the upper layers is dominant. These patterns are not detectable anymore, when switching to the vegetation productivity minimum.

The contrasting of the maps illustrating the normalized anomalies of the dominant variables during the extreme events (fig. 4c and 4d) reflects that dominant variables during maxima are usually positive and vice versa for minima. The normalized anomalies during maximum vegetation productivity indicate surpluses of dominant variables, especially in the areas of Mexico, east Africa and Australia. Contrary, the minimum vegetation productivity is characterized by deficits of dominant variables. Thus, maximum events are indicated by surpluses of their controlling variables, while minimum events are mainly dominated by deficits of their main drivers.

Through the fact that the analysis is averaged over three extremes, it is tried to minimize the chance that a certain variable is dominant because of simple coincidence. But simultaneously, the magnitude of the averaged hydro-meteorological anomalies is lowered in most cases. Hence, both of the maps display anomalies around $+/- 1$ over wide ranges.

Bringing together both maps for maximum vegetation productivity, the detected regions where soil moisture in shallow layers prevails, occur together with normalized anomalies with high positive magnitudes. In consequence, maximum vegetation productivity here was initiated by a surplus of soil moisture. Focusing

on the region in North Asia the energy-controlled as well as the water-controlled region are characterized by high positive anomalies. Thus, in energy-limited areas energy surpluses cause the maximum productivity of vegetation, while in water-limited water surplus does. In contrast, looking at the same region during minimum vegetation productivity, deficits of energy or water are constraining. Regarding the ratio of energy- versus water-limited regions, the barplots indicate during both extremes more water-limited regions than those more influenced by energy.

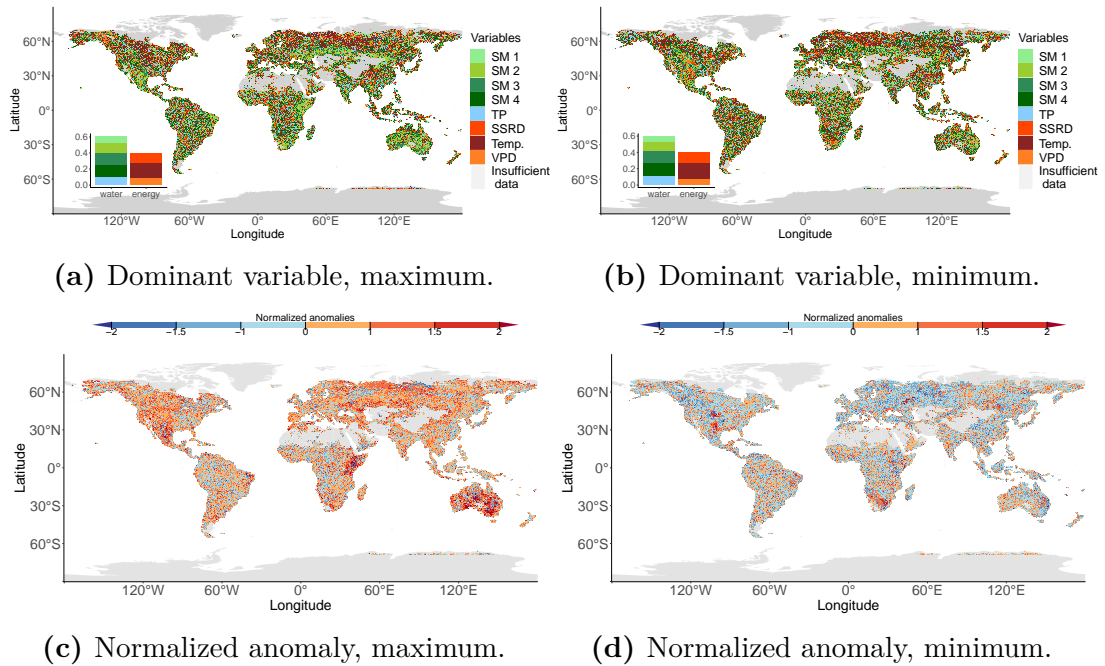


Figure 4: Dominant hydro-meteorological variable and its magnitude during extreme vegetation productivity.

3.3 Temperature-aridity plots, dominant variable

To expose the sensitivity of SIF extremes to hydro-meteorological variables according to long-term climate characteristics, all grid cells are sorted into boxes of the temperature-aridity plot. Within one box with a defined AI and long-term average temperature, the grid cells are grouped together by their dominant variable. Variables are assumed as dominant, when they are represented by the most grid cells in a box and therefore indicate the controlling factor for vegetation productivity in this climate type. They are displayed by the respective color.

These plots aggregate information across several climate regimes that correspond to the single boxes, and hence provide a more condensed illustration.

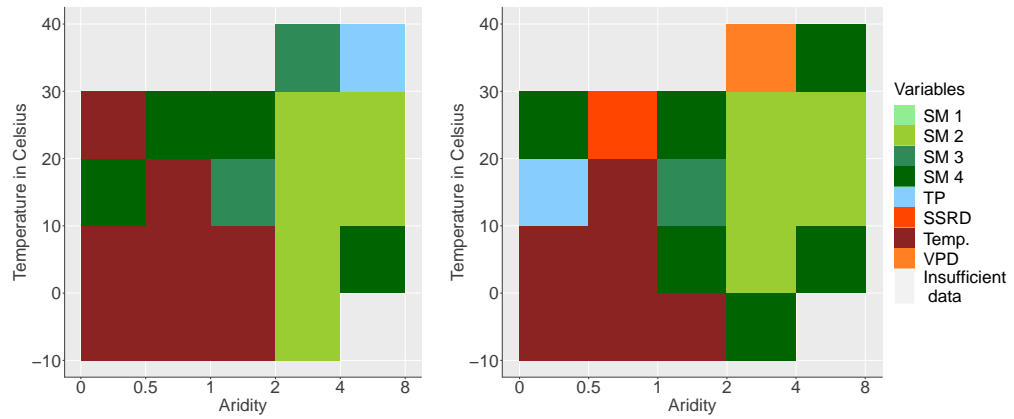
Like the global map, the temperature-aridity plot can also illustrate the magnitude of the controlling variable. Therefore, the median of normalized anomalies of all grid cells which represent the prevailing variable of the specific climate type is computed. The resulting value can be displayed on a color ramp, which serves to color the boxes.

To determine how representative the results are, it is decided to plot the percentage of grid cells representing the dominant variable.

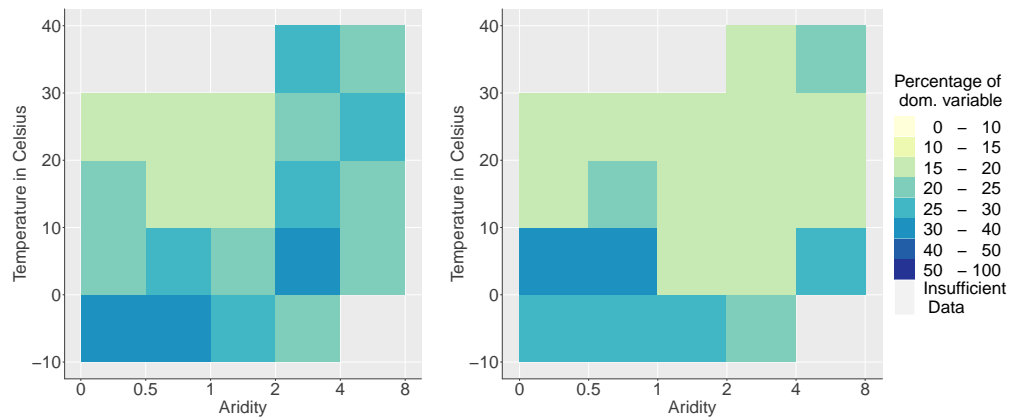
Fig. 5a indicates for vegetation productivity maximum, water variables in regions with an aridity larger than two (arid) as most controlling. Mainly soil moisture in layer 2 enhances vegetation productivity. In very warm arid regions, soil moisture in a deeper layer and precipitation become more dominant. In semi-arid regions the influence of hydro-meteorological variables depends on the mean temperature. If it is below 10°C , vegetation productivity is energy-controlled, above this threshold, water variables are the main drivers of productivity. However, in humid and semihumid regions energy-variables represent the strongest influences on vegetation productivity. But their controlling effects get weaker with increasing temperature, as in warm climate conditions also soil moisture in layer 4 controls maximum vegetation productivity.

Compared to the vegetation minimum in fig. 5b, the main patterns remain the same. But interestingly, there are also some climate boxes changing from energy to water control and vice versa. Also in the warm, arid regions VPD as an energy variable diminishes vegetation productivity, where in humid regions precipitation as water variable has a controlling character. Considering the normalized anomalies of the controls of minimum vegetation productivity in fig. 5f, reveals that precipitation in humid regions influences vegetation productivity negatively due to a high positive anomaly, the same accounts for VPD in warm, arid regions. Though, the percentage of grid cells in these climate types, which are controlled by these variables is between 15% to 20%, which is relatively low compared to other boxes in the temperature-aridity plot.

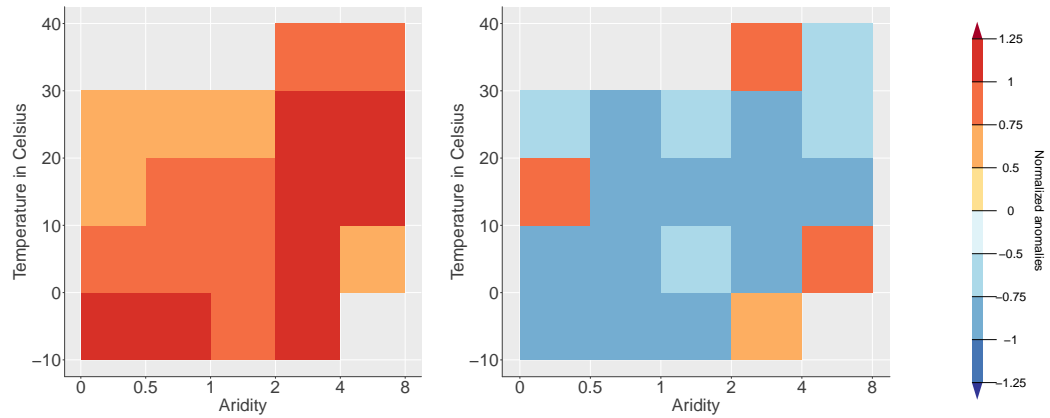
Also noteworthy is the fact that in a climate regime with a mean temperature between 0°C and 10°C and an aridity between 4 and 8 a positive soil moisture anomaly in layer 4 causes the maximum as well as the minimum of vegetation productivity, only the magnitude of the anomaly differs. This can also be seen for climate conditions with an average temperature between -10°C and 0°C .



(a) Dominant variable, maximum. (b) Dominant variable, minimum.



(c) Percentage with the dominant variable, maximum. (d) Percentage with the dominant variable, minimum.



(e) Normalized anomalies, maximum. (f) Normalized anomalies, minimum.

Figure 5: Temperature-aridity plots for extreme vegetation productivity.

Here, the soil moisture layer changes when comparing minimum and maximum productivity, but in both extremes a positive amount of soil moisture is causing the extreme.

While during maximum vegetation productivity a huge surplus of soil moisture in layer 2 is the largest co-occurring variable for 20 % to 30 % grid cells in several arid regions, a deficit of it could lead to the minimum productivity in those climate conditions. The latter is represented only by 15 % to 20 % of grid cells across different of the arid climate conditions.

The normalized anomalies plotted in fig. 5e and 5f strengthen the impression, which is gained from the global maps (fig. 4c and 4d). During maximum vegetation productivity there is a surplus of the controlling hydro-meteorological variables. In contrast, minimum productivity of vegetation is mainly driven by deficits of the dominant variables, except for the before mentioned exceptions.

For the maximum vegetation productivity it can be stated that the dominant variables plotted in fig. 5a are shared by more grid cells than the variables which are plotted for minimum vegetation productivity, as fig. 5c and 5d illustrate. This accounts especially for cold and arid regions. In both graphs climate regimes with a mean temperature between 10 °C to 30 °C, dominant variables are represented by a lower percentage of grid cells. For the maximum vegetation productivity this only pertains for climate regimes which are characterized by a long-term aridity below 2.

3.4 Temperature-aridity plots: second dominant variable

In this section the second most represented variable per box is displayed in the temperature aridity plots, the median of their normalized anomalies as well as the percentage of grid cells, which had this variable as most important. Fig. 6a and 6b illustrate the prevailing of deep soil moisture across all climate types. This impression is evoked by the illustration of both extremes. A clear border between arid and humid regions is not visible anymore. The percentage of grid cells showing this variables as most important is mainly between 10 % to 20 %. During maximum vegetation productivity in arid regions up to 25 % of all grid cells in the box have soil moisture in layer 3 as main driver. The normalized anomalies of the second most represented variable confirm the patterns seen for the most represented variable. The maximum vegetation productivity is mainly driven by surpluses, while deficits lead to the minimum of it.

During maximum vegetation productivity surpluses of deep soil moisture are the main drivers, except for cold, humid regions, where slight deficits occur.

Minimum vegetation productivity is mostly characterized by deficits of deep soil moisture. But in cold, arid regions and also in humid regions, surpluses of deep

soil moisture limit the vegetation functioning. The effect of dominant energy variables depends on the aridity, below 2 deficits of energy cause the minimum vegetation productivity, whereas above 2 a temperature surplus leads to it.

3.5 Difference between dominant and second-most represented variable

Finally, the percentages of first- and second-most represented variables are subtracted to reveal how representative the dominant variable of a certain climate type is. The differences of the percentages of first-most and second-most variables are displayed in fig. 7. If the differences are below 1 %, the most dominant variable is assumed as not representative.

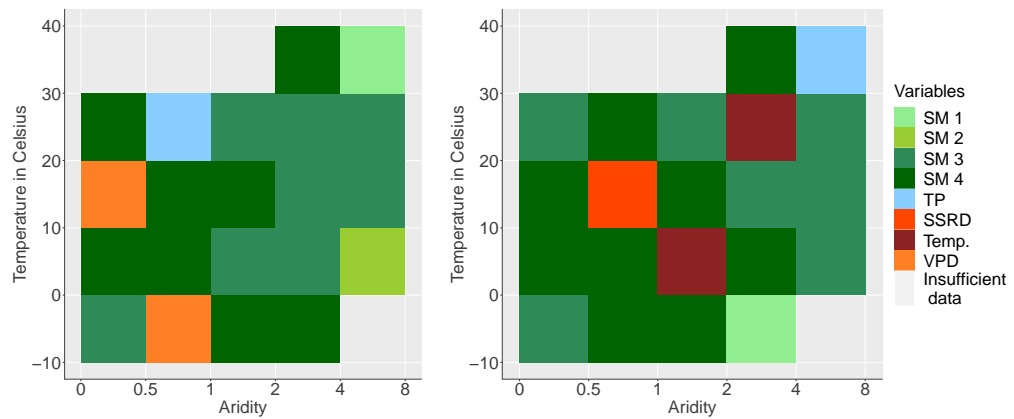
For a better comparison of dominant and second-most represented variables and the difference of their percentages, all graphs are displayed together in the attachments (fig. 10).

Especially in cold, humid regions the most represented variables are by far the dominant controls of vegetation productivity. In contrast, across warm climate regimes the difference between first and second most represented variable is much smaller. Particularly for the minimum vegetation productivity the most and second-most variable are similar often represented.

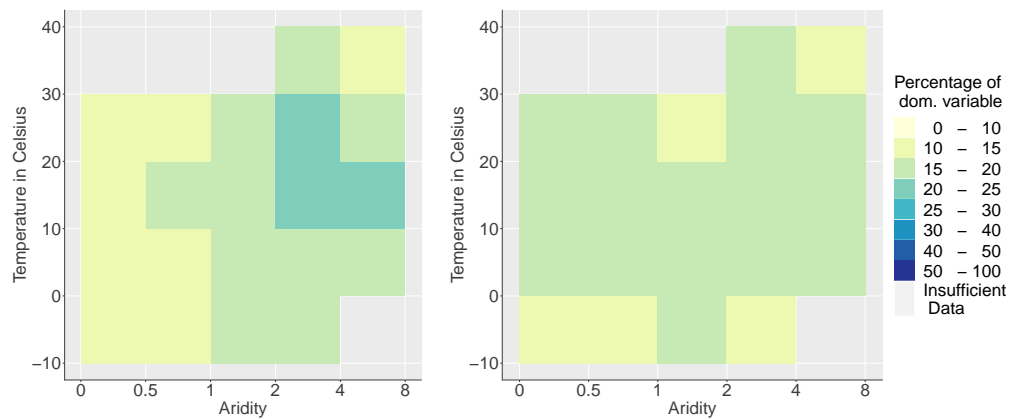
For maximum vegetation productivity differences occur under warm climate conditions. For example, in warm semihumid regions, the first dominant variable would not imply a shift from energy to water limitation when contrasting average to extreme productivity, but the second-most dominant does. The percentage difference states that in this climate regime the second dominant variable is being similar important, as the difference is less than 1 %. The second most represented variable is soil moisture layer 4, thus a shift from energy to water-limitation could be very likely.

Also in warm arid regions, first and second-most dominant variable have a very similar representation. Hence, the detected similarities between average and maximum vegetation productivity remain in the sense being water-controlled, but differ in the depth of soil moisture which is most important.

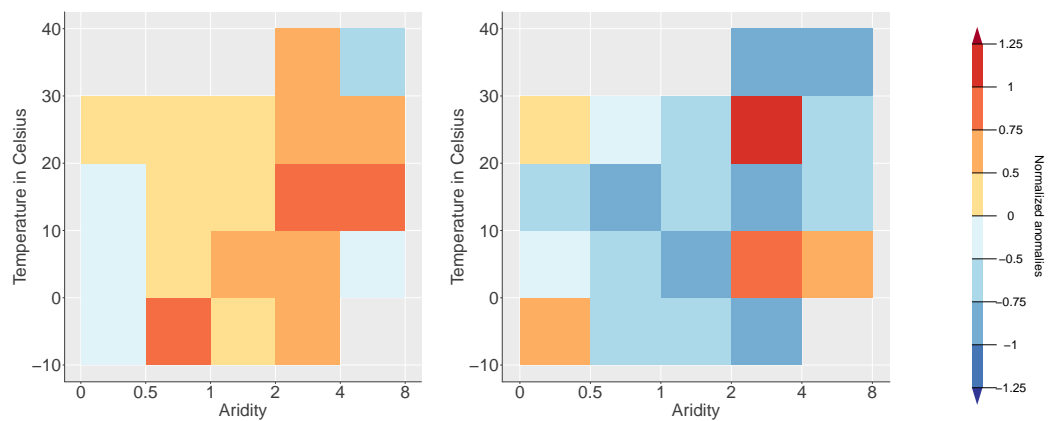
For the minimum vegetation productivity in warm regions the similarities of percentages of grid cells showing the most and second-most represented variable increase. In warm, humid regions the detected shifts from energy to water limita-



(a) Second dominant variable, maximum. (b) Second dominant variable, minimum.



(c) Percentage with the dominant variable, maximum. (d) Percentage with the dominant variable, minimum.



(e) Normalized anomalies, maximum. (f) Normalized anomalies, minimum.

Figure 6: Temperature-aridity plots for extreme vegetation productivity, second most represented hydro-meteorological variable.

tion when contrasting average and first-dominant variable can be confirmed by the second-most represented variable. The latter also indicates the dominance of water variables. So not only the most represented variable, but also the second-most represented one displays a shift from energy- to water-limitation in warm, humid regions.

However, also contradicting results can be deduced. During vegetation productivity minimum in semi-arid regions with a long-term average temperature between 0°C and 10°C the dominant variable suggests a shift from energy- to water limitation. Even so, the second dominant variable, which represents less than 1% less grid cells, does not show such a shift. In contrast, it illustrates the maintenance of water-limitation.

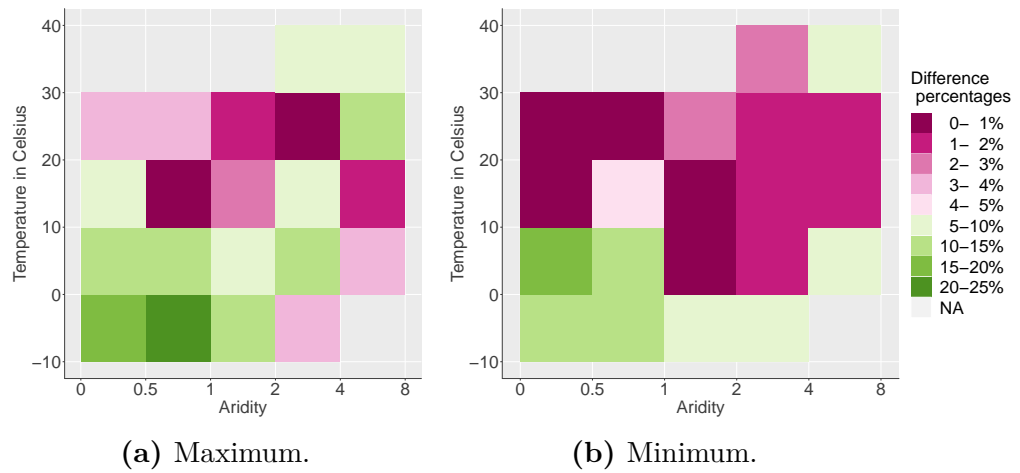


Figure 7: Difference between percentage of grid cells with most represented variable and second-most represented variable.

4 Discussion

In the following section, the deduced results are interpreted within the different categories from grid cell, over global maps to temperature-aridity plots.

4.1 Developments of hydro-meteorological variables before and after extreme vegetation productivity

From the figures 3a and 3b it can be derived that maximum vegetation productivity occurs while energy decreases and water availability increases. The different climate conditions would actually substantiate the hypothesis that Germany as a humid region is energy-limited and therefore a higher amount of energy would lead to a maximum vegetation productivity and vice versa for the Iberian Peninsula. With an aridity index of 0.84, Germany could also be counted as semihumid region. This would imply that Germany seasonally transitions between semihumid and semiarid conditions, what would partly explain the similarities with the development of variables on the Iberian Peninsula. Sticking with this assumption, an increase in soil moisture could benefit the vegetation towards a productivity maximum, what can be seen in the graph 3a.

The Iberian Peninsula is in the long term an arid region. Fig. 3b illustrates clearly how vegetation productivity increases, where VPD and temperature are strongly decreasing to almost zero. Assuming the Iberian Peninsula as an arid region with vegetation productivity being water-limited and enhanced by a surplus of water, is contradicted by the results of fig. 3b indicating soil moisture being lower than usual in all layers during maximum vegetation productivity. The assumption would suggest water variables show positive anomalies with large magnitude, when vegetation productivity is at its maximum. The simultaneous increase of water variables and decrease of energy variables might boost vegetation to its maximum productivity. It could also be possible that during bad persistent weather the grid cell has been energy-limited for a couple of months. Even so, the soil moisture development would not support this hypothesis, as it is lower than usual, implying that there has been less precipitation and more radiation.

However, focusing on minimum vegetation productivity both grid cells confirm the hypothesis of arid regions being water-controlled, whilst in humid regions energy variables dominate. Germany, as an example for humid regions experiences a vegetation productivity minimum due to low radiation and VPD. At the same time, water availability is higher. As Seneviratne et al. 2010 state, above a

critical level, evapotranspiration is no longer influenced by soil moisture but by energy. Understanding evapotranspiration as proxy for vegetation productivity, the minimum would thus be caused by low energy availability. Even so, according to the magnitude of the normalized anomalies, fig 3c could create the impression that soil moisture in upper layers is the main driver of minimum productivity, even if the grid cell is semihumid and thus water variables should not be the main co-variates. To evaluate this uncertainty, it is referred to the mean values of every variable after averaging over the three minimum vegetation productivity occurrences (tab. 2). Here, radiation is the most important variable, a results that supports the assumption of Germany being energy-limited and is in line with the findings of Seneviratne et al. 2010. Therefore, it is possible that the displayed grid cell and the dominance of soil moisture in this case might co-occur with the vegetation productivity minimum per coincidence.

The vegetation productivity minimum on the Iberian Peninsula occurs alongside minima in multi-layer soil moisture, corroborating the hypothesis that vegetation productivity in this grid cell is associated with water variables. They clearly indicate the largest magnitudes and hence are thought to display the most influencing variables. Finally, it can be concluded that those graphs are able to illustrate the development of hydro-meteorological variables and give insights on how vegetation productivity interacts with its drivers. But as they are based on one event, three out of four results show unexpected results, which is why their representative character may be limited.

4.2 Global maps

The regions detected in section 3.2 (Mexico, East Africa and Australia) state examples for dry, arid regions being mainly water-controlled during maximum vegetation productivity. This confirms the findings of W. Li et al. 2020 and X. Li and Xiao 2020, where vegetation in arid regions is dominated by water availability. Also, again considering evapotranspiration as proxy for vegetation productivity, the results of Denissen et al. 2020 and Seneviratne et al. 2010 emphasize, evapotranspiration being water-controlled in regions with dry soil. Thus, their results would also suggest a strong coupling of water availability and vegetation productivity in arid regions.

As the in section 3.2 presented maps illustrate dominant controls on vegetation productivity extremes, a comparison with a map of dominant controls on average vegetation productivity could reveal certain differences. Fig. 8 shows the latter

ones. The used data for this graph are half-monthly SIF values, ranging from 2007-2018 with a $0.5^\circ \times 0.5^\circ$ spatial scale. Hence, the plotted data only differs in temporal resolution, time period of data and the way of detrending it. All other characteristics match, making the global maps comparable. In general, fig. 8 shows much stronger spatially cohesive patterns, suggesting average vegetation productivity being more equally controlled in adjacent grid cells than extreme productivity. Also, it has to be considered, that the variables co-occurring with average vegetation productivity are calculated over much more time points than the variables associated with extreme vegetation productivity, as the latter are only computed out of three events. Contrasting the barplots of energy- and water-limitation between average and extreme conditions, a slight change in the direction of water-controlling can be detected for the extremes.

The prevailing from soil moisture in layer 2 in water-limited regions is outstanding (8). Relics of these patterns can be found in the maximum vegetation productivity map, for example in Mexico, East Africa, Australia and central Russia.

Clear changes are visible when comparing south Africa and southern mid-US in the minimum vegetation productivity map to the map of W. Li et al. 2020. During the minimum, energy variables are main drivers of vegetation productivity, while under average conditions shallow soil moisture controls it. Hence, here shifts from water-limited to energy-limited conditions are detectable. The combination of fig. 4b and 4d reveals high anomalies of temperature and VPD as dominant control of the vegetation minimum productivity. The increasing restrictive effects of high VPD on vegetation functioning due to an increase in temperature are also clearly stated by Novick et al. 2016.

Both extreme vegetation productivity maps indicate a clear transition between energy- and water limitation in Russia. The results of Flach et al. 2018, analysing the Russian heat wave of 2010, confirm the presence of this border. In their study, different reactions of the biosphere were detected. The part north of the transition zone experienced a higher gross primary production, while the part below had a diminished gross primary production. This is in line with the patterns displayed fig. 4a and 4b. In the northern part of Russia, the maximum vegetation productivity is associated with energy surpluses. Hence, a heatwave would cause an energy surplus, which may lead to the increasing vegetation productivity. In contrast, in the region south of the border, minimum vegetation productivity co-varies with water deficits, which could be triggered by a heatwave, and therefore leading to less gross primary production.

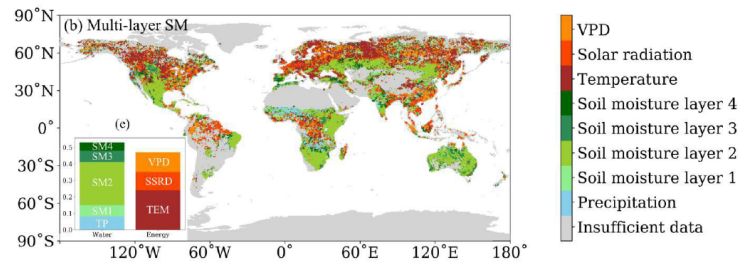


Figure 8: Dominant variables for average vegetation productivity (W. Li et al. 2020).

4.3 Temperature-aridity plots

The previous section already stated differences in controlling hydro-meteorological variables between different regions. The temperature-aridity plots of the dominant variables confirm these results. In arid climate conditions water variables limit or enhance vegetation productivity, while in humid climate conditions energy variables prevail. In regions with an aridity index between 1-2, the controlling elements of maximum vegetation productivity differ along a temperature gradient. Above 10 °C temperature is not anymore the main driver, instead deep soil moisture prevails. This change from energy to water-limitation with increasing temperatures could be due to the dependency of vegetation productivity on an optimal temperature. Huang et al. 2019 find average optimal temperatures ranging globally between 10 °C and 30 °C. As cold, semiarid regions have not reached the lower limit of this range, this might explain the strong impact of temperature on vegetation productivity in those climate regimes.

During vegetation productivity minimum, fig. 5b shows water variables associated with actually energy-limited regions and VPD co-varying with vegetation in water-limited climate conditions. This might disagree with the general assumption that evapotranspiration as proxy for photosynthesis is water-controlled in dry regions and energy-controlled in wet regions (Denissen et al. 2020; Seneviratne et al. 2010). But, there could also be a strong coupling between the certain energy and water variables. Liu et al. 2020 highlight in their study that VPD can just reduce vegetation productivity if a strong coupling with soil moisture is assumed. Therefore, the high VPD causing the vegetation productivity minimum might co-occur with a low availability of soil moisture, which would match the overall patterns and is line with the results of Denissen et al. 2020; Seneviratne et al. 2010.

An explanation for the negative influence of high precipitation on vegetation

productivity in humid regions could be given by Roderick et al. 2001. Here, the authors state that clouds have a huge reducing influence on the proportion of direct radiation, which reaches the surface and is therefore usable for vegetation. As high precipitation is linked to the occurrence of clouds, one could also assume a link between high precipitation and low radiation and hence reduced vegetation productivity in humid regions. For the explanation of precipitation surpluses co-varying with vegetation productivity minimum in humid regions, this would mean high positive precipitation anomalies reduce vegetation productivity through decreasing the amount of radiation reaching the surface.

Comparing the extreme productivity controls to those of average vegetation productivity in fig. 9 several differences become visible. Maximum vegetation productivity in warm humid regions is associated with soil moisture in layer 4, whereas the driver of average productivity within those climate conditions is radiation, so a shift from energy to water limitation can be deduced. Additionally, vegetation productivity in those climate regimes is no longer increased by radiation but through temperature. Across all climate types, an association between increasing deep soil moisture and vegetation productivity maximum can be detected. To further interpret these co-variations regarding their causes, information about the vegetation type and its rooting depth would be needed. Therefore, dominant variables could be displayed in an rooting depth- or vegetation cover-aridity plot. Positive soil moisture in layer 4 co-variates with both extremes, so the same occurrence has contrary effects on vegetation productivity. Only the magnitude of anomalies differs. Regarding to the Feddes model (Feddes, Kowalik, and Zaradny 1978) it could be assumed, that surplus associated with maximum vegetation productivity is within the content of soil moisture benefiting vegetation productivity. While the surplus, which leads to the minimum could be so large, that soil moisture is limiting vegetation productivity (Feddes, Kowalik, and Zaradny 1978). For vegetation productivity minimum shifts from energy to water limitation occur in warm, humid regions and temperature is partly replacing radiation as dominant control. Furthermore, in the semi-arid regions the transition from climate conditions where water prevails to those where energy prevails is shifted into colder regions. Now, low deep soil moisture in regions with a mean temperature between 0°C and 10°C diminishes vegetation productivity the most. The explanation of Huang et al. 2019 that there is an optimal temperature for vegetation productivity can be applied to explain maximum vegetation productivity in those climate conditions. But for vegetation productivity minima temperature is not anymore

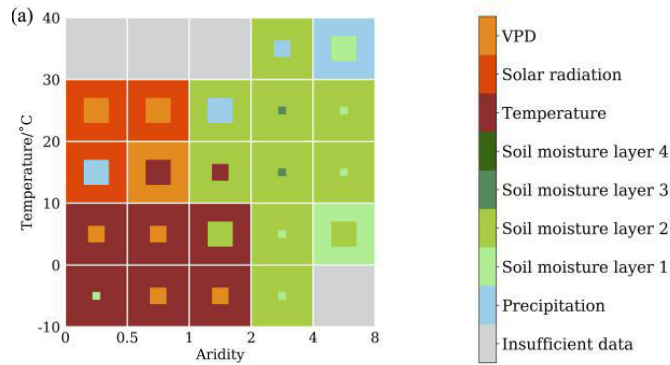


Figure 9: Temperature-aridity plot of the controlling variables for average vegetation productivity (W. Li et al. 2020).

the most co-varying variable.

4.4 Second-most dominant variable and differences to the dominant variable

On the one hand the illustrations of the second most dominant variables for both extremes confirms several changes from energy- to water limitation, as those shifts are not only seen for the most represented but also for the second most represented variable. On the other hand, they also reveal limits of the analysis. In some cases, first and second-dominant variables had almost the same percentage of grid cells, but shifts between water- and energy-control detected with the first dominant variable contradict with drivers of vegetation productivity represented by the second-most dominant variable. For example, the most represented variable shows a change from energy- to water-limitation, but this is not seen for the second most represented variable, even if they have similar high percentages of grid cells within the climate regime. This insight is very useful as it highlights the need for further investigations and calculations to indicate the robustness of the determined variables, which co-occur with vegetation productivity extremes. At the same time it is emphasized that there is not necessarily causality between the most dominant variables and vegetation productivity, but that only the largest anomalies of hydro-meteorological variables co-variate with vegetation productivity extremes.

5 Conclusion

After analyzing single grid cells, global maps and in the end different climate conditions, four major points can be stated regarding to co-variations between hydro-meteorological variables and vegetation productivity extremes:

- Vegetation productivity maxima are associated with surpluses of the prevailing variables, while minima co-occur with deficits of hydro-meteorological variables.
- Deep soil moisture shows an increasing importance during extreme vegetation productivity.
- Shifts from energy- to water-limitation and vice versa can be detected, when contrasting average to extreme vegetation productivity.
- The robustness of these shifts has to be figured out, as in some cases second-most represented variables are dominant in a similar number of grid cells.

For a further interpretation, the results could be linked to vegetation parameters within the different regions like tree cover and root depth. This could benefit a better understanding, why deep soil moisture gains importance. Also, the variables with the second largest normalized anomaly in grid cells could be plotted. This would offer the possibility to check the couplings mentioned in the discussion, like precipitation-radiation or soil moisture-VPD.

Especially, the last two findings indicate the importance to remember that the shown results represent associations between variables and vegetation productivity, but not necessarily causalities between the variables and vegetation productivity. To state this, further investigations are needed.

Attachments

Comparison of first and second-most represented variable

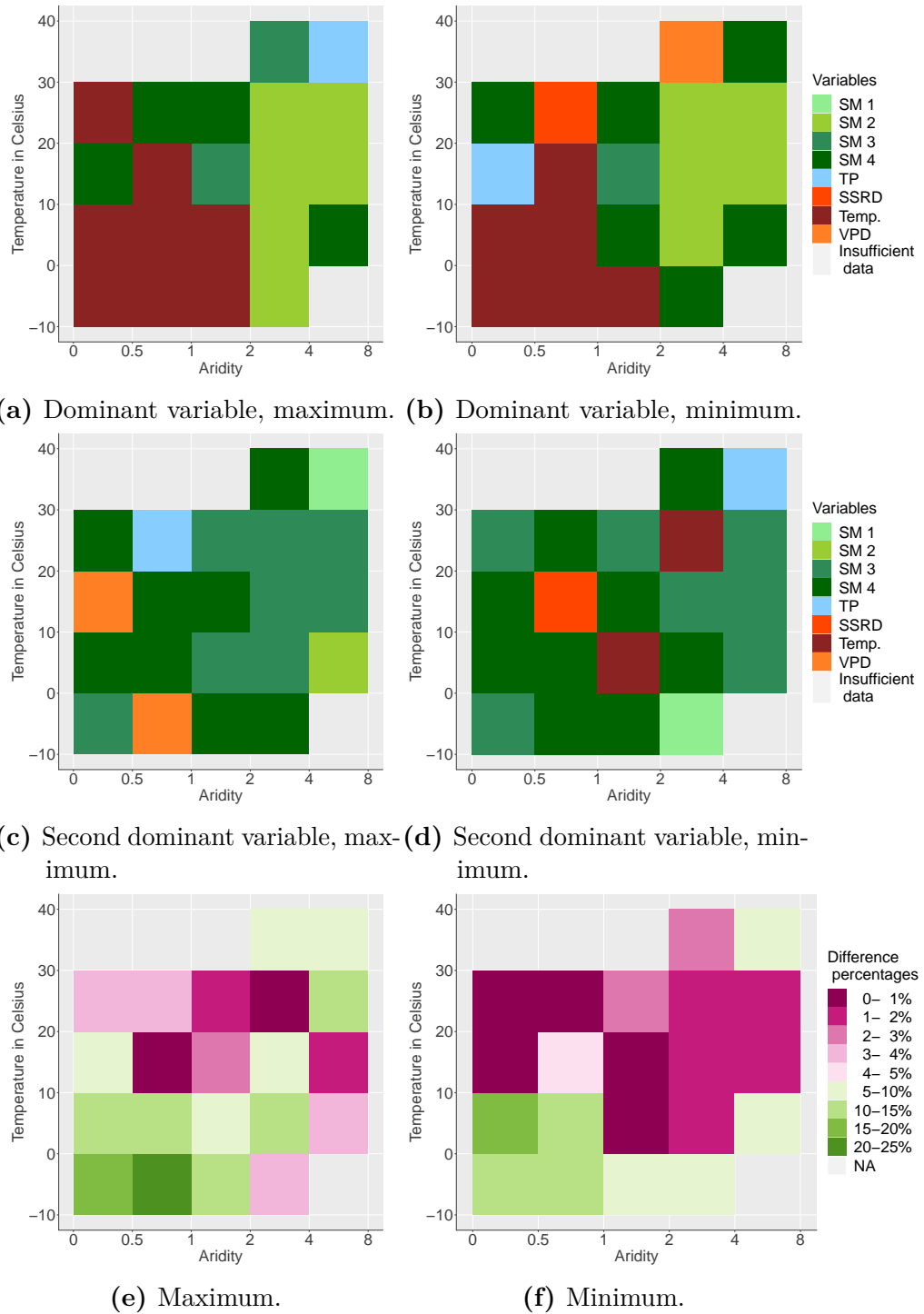


Figure 10: First and second dominant variables in various climate conditions and the difference between percentages of grid cells representing them.

References

- (C3S), Copernicus Climate Change Service (2017). *ERA5: Fifth generation of ECMWF atmospheric reanalyses of the global climate*. <https://cds.climate.copernicus.eu/cdsapp#!/home>. Copernicus Climate Change Service Climate Data Store (CDS), date of access: 15-11-2019.
- Denissen, Jasper MC, Adriaan J Teuling, Markus Reichstein, and René Orth (2020). “Critical soil moisture derived from satellite observations over Europe”. In: *Journal of Geophysical Research: Atmospheres* 125.6, e2019JD031672.
- Feddes, RA, PJ Kowalik, and H Zaradny (1978). “Water uptake by plant roots”. In: *Simulation of field water use and crop yield*, pp. 16–30.
- Flach, Milan, Sebastian Sippel, Fabian Gans, Ana Bastos, Alexander Brenning, Markus Reichstein, and Miguel D Mahecha (2018). “Contrasting biosphere responses to hydrometeorological extremes: revisiting the 2010 western Russian heatwave”. In: *Biogeosciences* 16, pp. 6067–6085.
- Hansen M., X. Song. (2018). *Vegetation Continuous Fields (VCF) Yearly Global 0.05 Deg.[VCF5KYR]*. <https://doi.org/10.5067/MEaSURES/VCF/VCF5KYR.001>.
- Huang, Mengtian, Shilong Piao, Philippe Ciais, Josep Peñuelas, Xuhui Wang, Trevor F Keenan, Shushi Peng, Joseph A Berry, Kai Wang, Jiafu Mao, et al. (2019). “Air temperature optima of vegetation productivity across global biomes”. In: *Nature ecology & evolution* 3.5, pp. 772–779.
- Joiner, J, Luis Guanter, R Lindstrot, M Voigt, AP Vasilkov, EM Middleton, KF Huemmrich, Y Yoshida, and C Frankenberg (2013). “Global monitoring of terrestrial chlorophyll fluorescence from moderate spectral resolution near-infrared satellite measurements: Methodology, simulations, and application to GOME-2”. In: *Atmospheric Measurement Techniques* 6.2, pp. 2803–2823.
- Köhler, Philipp, Luis Guanter, and Joanna Joiner (2015). “A linear method for the retrieval of sun-induced chlorophyll fluorescence from GOME-2 and SCIAMACHY data”. In: *Atmospheric Measurement Techniques* 8, pp. 2589–2608.
- Li, Wantong, Mirco Migliavacca, Matthias Forkel, Sophia Walther, Markus Reichstein, and René Orth (2020). “Revisiting global vegetation controls using multi-layer soil moisture”. In: *Earth and Space Science Open Archive (ESSOAr)*.
- Li, Xing and Jingfeng Xiao (2020). “Global climatic controls on interannual variability of ecosystem productivity: Similarities and differences inferred from

- solar-induced chlorophyll fluorescence and enhanced vegetation index”. In: *Agricultural and Forest Meteorology* 288-289, p. 108018.
- Liu, Laibao, Lukas Gudmundsson, Mathias Hauser, Dahe Qin, Shuangcheng Li, and Sonia I Seneviratne (2020). “Soil moisture dominates dryness stress on ecosystem production globally”. In: *Nature communications* 11.1, pp. 1–9.
- Novick, Kimberly A, Darren L Ficklin, Paul C Stoy, Christopher A Williams, Gil Bohrer, A Christopher Oishi, Shirley A Papuga, Peter D Blanken, Asko Noormets, Benjamin N Sulman, et al. (2016). “The increasing importance of atmospheric demand for ecosystem water and carbon fluxes”. In: *Nature climate change* 6.11, pp. 1023–1027.
- Qiu, Bo, Jun Ge, Weidong Guo, Andrew J Pitman, and Mengyuan Mu (2020). “Responses of Australian Dryland Vegetation to the 2019 Heat Wave at a Subdaily Scale”. In: *Geophysical Research Letters* 47.4, e2019GL086569.
- Roderick, Michael L, Graham D Farquhar, Sandra L Berry, and Ian R Noble (2001). “On the direct effect of clouds and atmospheric particles on the productivity and structure of vegetation”. In: *Oecologia* 129.1, pp. 21–30.
- Seneviratne, Sonia I, Thierry Corti, Edouard L Davin, Martin Hirschi, Eric B Jaeger, Irene Lehner, Boris Orlowsky, and Adriaan J Teuling (2010). “Investigating soil moisture–climate interactions in a changing climate: A review”. In: *Earth-Science Reviews* 99.3-4, pp. 125–161.
- Wang, Xiaorong, Bo Qiu, Wenkai Li, and Qian Zhang (2019). “Impacts of drought and heatwave on the terrestrial ecosystem in China as revealed by satellite solar-induced chlorophyll fluorescence”. In: *Science of The Total Environment* 693, p. 133627.
- Zhang, Lifu, Na Qiao, Changping Huang, and Siheng Wang (2019). “Monitoring drought effects on vegetation productivity using satellite solar-induced chlorophyll fluorescence”. In: *Remote Sensing* 11.4, p. 378.

Statement of authorship

I declare that I have prepared this thesis independently and only with the use of the indicated sources. Direct and indirect quotations are marked as such. The submitted work has not been used elsewhere as an examination performance or published in German or another language as a publication.

Jena, January 22, 2021

Josephin Kroll